

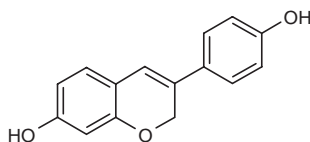
Idronoxil

Rec INN; USAN

Phenoxodiol NV-06

3-(4-Hydroxyphenyl)-2H-1-benzopyran-7-ol

InChI=1/C15H12O3/c16-13-4-1-10(2-5-13)12-7-11-3-6-14(17)8-15(11)18-9-12/h1-8,16-17H,9H2



C₁₅H₁₂O₃

Mol wt: 240.254

CAS: 81267-65-4

EN: 273285

Abstract

Idronoxil (phenoxodiol) is being developed as a novel anticancer therapeutic both as a single agent and as a chemosensitizer in late-stage cancers resistant or refractory to other approved chemotherapies. Idronoxil targets dysregulated prosurvival pathways mediated via Akt, FLIP and XIAP in cancer cells, restoring caspase-mediated apoptosis. Pharmacological studies demonstrated that idronoxil was able to sensitize cancer cells to a range of cytotoxic agents, and in particular to potentially sensitize platinum-resistant ovarian cancer cells. Further studies have demonstrated that idronoxil also possesses antiangiogenic properties. Idronoxil has been evaluated in several clinical studies, with the major adverse events being low-grade nausea, minor hypersensitivity reactions and transient thrombocytopenia when delivered i.v., attributed to the cyclodextrin excipient used in that formulation. For orally delivered idronoxil, an MTD of 800 mg t.i.d. was observed, manifesting as mild diarrhea in a small number of patients. Idronoxil has demonstrated efficacy as monotherapy in phase II studies in late-stage hormone-refractory prostate cancer, and as a chemosensitizing agent in platinum-resistant ovarian cancer when used in combination with cisplatin and paclitaxel. Idronoxil is currently being evaluated in a phase III multicenter, randomized, double-blind trial in platinum-resistant or -refractory late-stage epithelial ovarian, fallopian or primary peritoneal cancer patients following at least second-line platinum therapy, as an oral formulation in combination with carboplatin.

Synthesis

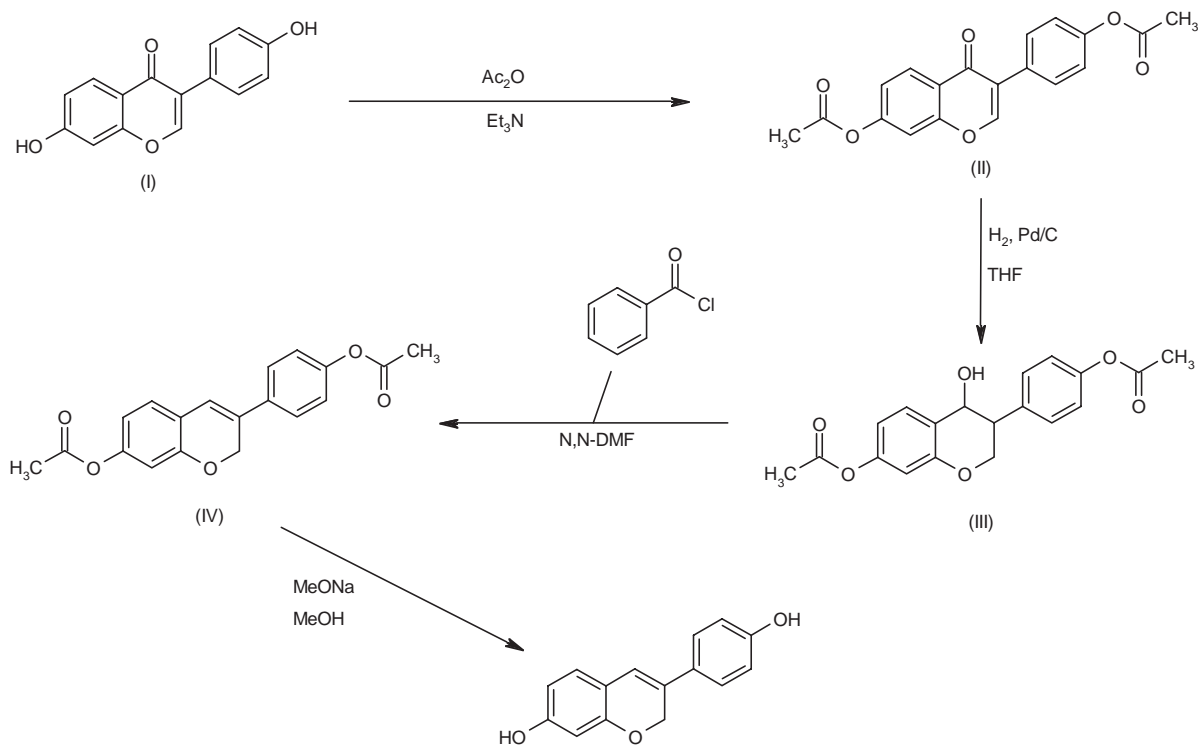
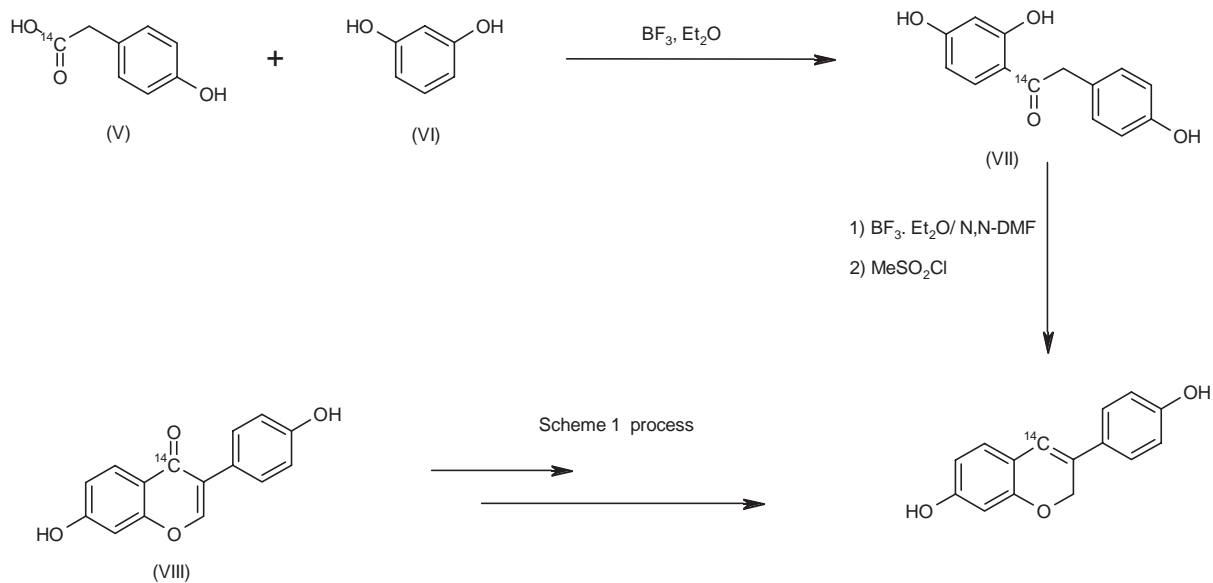
Idronoxil is synthesized by a linear synthetic strategy starting from either very simple starting materials or from commercially available highly elaborated intermediates. The availability of this intact carbon scaffold allows for a simple functional group modification synthetic strategy. The key highly elaborated intermediate daidzein (I) is protected as the bis-acetate using acetic anhydride and triethylamine. Diacetyldaidzein (II) is smoothly reduced to diacetyltetrahydrodaidzein (III) by catalytic heterogeneous low-pressure hydrogenation. Diacetyltetrahydrodaidzein is dehydrated efficiently by benzoyl chloride in refluxing dimethylformamide. The resulting diacetyldehydroequol (IV) is deacetylated by sodium methoxide in methanol to afford idronoxil in high yield. Scheme 1.

Daidzein is a readily available starting material and affords a very cost-effective and efficient means of synthesizing idronoxil. In order to complete advanced ADME studies, labeled idronoxil was prepared. [¹⁴C]-Labeled idronoxil was prepared from [¹⁴C]-labeled 4-hydroxyphenylacetic acid. The condensation of labeled 4-hydroxyphenylacetic acid (V) with resorcinol (VI) was completed using boron trifluoride diethyletherate. The resulting labeled benzoin (VII) was cyclized using modified Haak conditions: boron trifluoride in dimethylformamide with methanesulfonyl chloride. The resulting labeled daidzein (VIII) was then progressed through the standard protection–hydrogenation–dehydration–deprotection strategy to afford labeled idronoxil. Scheme 2.

Background

Idronoxil (phenoxodiol) is an analogue of the naturally occurring plant isoflavone genistein. Genistein is a pan-protein tyrosine kinase inhibitor, inducing mitotic arrest, terminal differentiation and apoptosis of human cancer

Scheme 1: Synthesis of Idronoxil

Scheme 2: Synthesis of [^{14}C]-Idronoxil

cells (1-4). Steric alteration of the genistein scaffold to create idronoxil yielded a compound that has considerably greater anticancer activity, improved absorption and substantially different pharmacology, while retaining the good safety profile of its naturally occurring analogue.

Idronoxil belongs to a class of drugs known as multiple signal transduction regulators ("MSTRs"). Malfunctions in key components of the signal transduction process (whereby a series of chemical signals within a cell lead to the expression of a particular function) are fundamental to neoplastic transformation, leading to cancer, where cells respond abnormally to survival signals. The molecular components of these regulatory pathways are interconnected, thereby maintaining a delicate balance between the life and death of a cell; however, modulation of these intrinsic elements in cancer cells tips the balance toward survival, resulting in a neoplastic event and cancer onset (5, 6). Restoring the normal balance by inhibiting survival pathways is the major objective of new therapeutic compounds such as idronoxil.

Idronoxil elicits its broad anticancer activity via the following mechanisms (7):

- Modulation of both pro- and antiapoptotic proteins of the extrinsic and intrinsic programmed cell death pathways
- Degradation of XIAP and Akt
- Cell cycle arrest
- Antiangiogenesis

Preclinical Pharmacology

In epithelial ovarian cancer cells (EOC), idronoxil-induced apoptosis is caspase-3-dependent and proceeds via both extrinsic (death receptor) and intrinsic (mitochondrial) pathways (7). Idronoxil has been shown to specifically downregulate both the phosphorylation status and expression of Akt, resulting in increased degradation of X-linked inhibitor of apoptosis (XIAP) and the short version of FLIP (8). Idronoxil-induced degradation of the death receptor inhibitor FLIP enables death receptor-mediated cleavage of procaspase-8 to its active form, thereby resulting in the activation of the extrinsic apoptotic pathway. Indeed, pretreatment of Fas-refractory EOC cells with idronoxil restores their sensitivity to agonists of the Fas/FasL extrinsic apoptotic pathway (9). Activation of caspase-8 and degradation of XIAP also enables apoptosis to proceed by the intrinsic pathway via BID cleavage and caspase-9 activation. Idronoxil-mediated activation of the intrinsic apoptotic pathway is also thought to be due to mitochondrial depolarization induced by conformational changes in Bax on the mitochondrial membrane and by caspase-2-catalyzed truncation of BID (8).

Further work on the mechanisms by which XIAP is degraded has shown that accompanying the decrease in XIAP is a subsequent decrease in phosphorylated Akt (p-Akt) and a decrease in total Akt occurring between 8 and 16 h. The appearance of the p30 XIAP fragment at 16 and 24 h is thought to be due to its cleavage by activated caspase-3, -8 and -9. XIAP is a known substrate for

the serine protease OMI/HtrA2, which is released from the mitochondria about 8 h following idronoxil treatment, thereby potentially contributing to the production of the p30 XIAP fragment. Concurrent with cytochrome *c* and OMI/HtrA2 release from mitochondria and accumulation in the cytosol, another mitochondrial protein, second mitochondria-derived activator of caspase (Smac), or direct IAP-binding protein with low pI (Diablo), was also found to be released in response to idronoxil some 8 h posttreatment. Rather than cleaving XIAP, Smac/Diablo promotes apoptosis by sequestering XIAP, thereby preventing its inhibition of the caspases (8). Taken together, the idronoxil-mediated release of OMI/HtrA2 and Smac/Diablo from the mitochondria to the cytosol further contributes to the inactivation of XIAP and overall reactivation of programmed cell death. Similar studies have also demonstrated that idronoxil induced XIAP degradation and activated caspases in platinum-resistant explants derived from melanoma patients. The authors concluded that idronoxil-induced XIAP degradation was responsible for the resensitization of these cells to carboplatin (10).

Modulation of the sphingomyelin pathway also has a key role in idronoxil-induced toxicity in cancer cells. The overproduction of sphingosine 1-phosphate (S1P) by a dysregulated sphingomyelinase pathway and sphingosine kinase (SK) in cancer cells is known to impart positive feedback on prosurvival cell signaling via Akt stabilization, resulting in apoptosis suppression (6, 11-13). Conversely, ceramide production by sphingomyelinase is known to promote G1 cell cycle arrest and induce caspase-mediated apoptosis (14-16). Idronoxil was shown to inhibit the production of S1P and promoted ceramide accumulation in cervical cancer HeLa cells (17). Furthermore, idronoxil treatment of head and neck (KB-3-1), ovarian (A2780) and doxorubicin-resistant breast cancer cells (MCF7/ADR) resulted in an accumulation of intracellular ceramide in these cell lines (18). Conversely, while S1P production in human endothelial cells (an example of a noncancer cell line) was inhibited by idronoxil following induction with tumor necrosis factor α (TNF- α), there was no effect on the basal activity of the enzyme, which suggests that idronoxil may impart post-translational or transcriptional control over SK activity in normal cells when these cells are stimulated (19).

Additional investigations on upstream mediators, based on the initial results of studies at Purdue University and independent studies at the Malaghan Institute of Medical Research at Victoria University, Wellington, New Zealand, suggest that a family of surface oxidases may represent the putative primary molecular target of idronoxil. Idronoxil inhibition of this family of surface oxidases, NADH-oxidoreductases expressed on the outer cell membrane (ECTO-NOX), has been shown to increase the plasma membrane content of ubiquinol, which in turn results in cytosolic accumulation of NADH and the resulting decoupling of the S1P prosurvival signal transduction cascade, which may then lead to inhibition of Akt, XIAP and FLIP (17, 20). Idronoxil-induced inhibition

of these surface oxidases also results in an accumulation of ceramide due to activation of plasma membrane sphingomyelinase (20). Both events (concurrent reduction in S1P and accumulation of ceramide) appear to initiate caspase-3-dependent programmed cell death. This family of surface oxidases is preferentially expressed on abnormally proliferating cells, such as cancer cells, which explains the apparent targeted toxicity of idronoxil for cancer cells and the lack of effect on normal cells.

Idronoxil is able to disrupt the cell cycle in the majority of cancer cell lines assessed to date. The phase (S, G1 and G2M) and potency of cell cycle arrest are dependent on cell type, idronoxil concentration and duration of exposure. Idronoxil strongly blocks cycling of A2780 ovarian cancer cells at the S phase, with a more moderate block at G2M (21). Idronoxil was shown to arrest the cell cycle in head and neck squamous cell carcinoma cell lines in G1 by 12 h, with a concomitant decrease in S phase using both bivariate distribution analysis in bromodeoxyuridine (BrdU)-positive cells and propidium iodide-stained cells analyzed by DNA histogram. Idronoxil elicited this effect by inhibiting CDK2 activity due to increased p21WAF1 expression independently of p53 (22).

In addition to idronoxil's direct effects on cancer cell survival, the agent also inhibits angiogenesis, as determined by *in vitro* and *in vivo* studies. Idronoxil inhibits the proliferation and migration of human endothelial cells in a cellular model of wound healing, without evidence of cytotoxicity. At the molecular level, idronoxil downregulates the expression of matrix metalloproteinase MMP-2 mRNA and inhibits the surface expression of adhesion molecules following TNF- α treatment in human endothelial cells. In an *in vivo* model of angiogenesis using the CBA mouse, idronoxil inhibited the penetration of vessels into the drug-infused gel foam sponge after subcutaneous (s.c.) implantation (19).

Apart from the efficacy of idronoxil as monotherapy, it is able to sensitize a broad range of cancer cell lines to various cytotoxic agents (Table I) (8, 23, 24). Of the idronoxil-drug combinations assessed, the agent synergized strongly with cisplatin, paclitaxel, gemcitabine and doxorubicin against ovarian and pancreatic cancer cells. Idronoxil was effective at chemosensitizing ovarian cancer cells to cisplatin, gemcitabine, paclitaxel, camptothecin and doxorubicin, pancreatic cancer cells to cisplatin, gemcitabine and doxorubicin, and prostate cancer cells to paclitaxel. In the case of idronoxil combinations with cisplatin, paclitaxel and doxorubicin against A2780 subline CP70 cells and idronoxil combinations with gemcitabine and doxorubicin against human pancreas HPAC cells, the sequence of administration did not affect the degree of synergistic toxicity.

Further studies have been conducted using combination index (CI) analysis (25) of synergy and revealed that idronoxil sensitizes both platinum-resistant (CP70) and -sensitive (A2780) ovarian cancer cells to cisplatin and carboplatin (Fig. 1). CI testing of drugs was done directly (i.e., concurrent exposure) or in sequence (sequential exposure). We observed that optimal sensitization of all

cells required a 24-h pretreatment with idronoxil at varying concentrations, followed by a 120-h treatment with either platinum drug. Concurrent exposure of cells to idronoxil and either platinum agent did result in some synergy, although the degree of synergy was less pronounced when compared to sequential exposure (Table I).

Reversal of the sequence (platinum followed by idronoxil) has not been assessed by CI, although using IC₅₀ comparison and a 3D model of synergy (26) this sequence of exposure resulted in mainly additive effects (data not shown). When increasing idronoxil concentrations were used in combination with carboplatin (200 mM) or cisplatin (25 mM), idronoxil induced clear concentration-dependent enhancement of the cytotoxicity of both platinum agents against the platinum-resistant CP70 cell line. Using CI, synergy (CI < 1) was observed using the higher-dose idronoxil-platinum drug combinations (i.e., 3.25 or 6.25 mM idronoxil + 200 mM carboplatin; 6.25 or 12.5 mM idronoxil + 25 mM cisplatin) (Fig. 1A and B). At these concentrations, the dose reduction index (reduction in the effective dose of platinum as monotherapy) to achieve 90% cell kill when used in combination with idronoxil was 4-fold for carboplatin and 5-fold for cisplatin. Similar results were obtained using both the idronoxil-cisplatin and idronoxil-carboplatin combinations against the platinum-susceptible A2780 cell line, only much lower concentrations of both combinations of idronoxil and either of the platinum agents were required to achieve similar cell kill at the IC₉₀. A dose reduction index of 4-fold was achieved using idronoxil and carboplatin at the concentrations employed and of ~30 fold using the idronoxil-cisplatin combination against the A2780 cell line (Fig. 1C and D).

These data demonstrate that idronoxil effectively sensitizes both platinum-resistant and -susceptible ovarian cancer cell lines to both carboplatin and cisplatin. When assessed against normal neonatal foreskin fibroblast (NFF) cell lines using the 3D analysis of synergistic toxicity, there was no evidence that idronoxil augmented platinum cytotoxicity (data not shown).

Proof-of-concept studies in ovarian cancer xenograft models confirmed that idronoxil is able to augment the toxicity of the platinum agents, gemcitabine, paclitaxel and topotecan (Table II). Cisplatin and idronoxil dosed in combination (idronoxil 10 mg/kg s.c. q3d \times 4 and cisplatin 0.5 mg/kg s.c. q3d \times 4) significantly retarded A2780 xenograft tumor growth at a level exceeding that observed in animals dosed with cisplatin (1 mg/kg) or idronoxil (20 mg/kg) as monotherapy using the same route of administration and regimen (%T/C = 17.4 vs. 31.8 and 29.2, respectively). In the CP70 ovarian cancer xenograft model, gemcitabine and idronoxil dosed in combination (idronoxil 50 mg/kg p.o. once daily and gemcitabine 1 mg/kg i.p. q3d \times 4) significantly retarded tumor growth at a level exceeding that observed in animals dosed with gemcitabine (2 mg/kg) or idronoxil (100 mg/kg) alone using the same route of administration and regimen (%T/C = 12.8 vs. 20.3 and 87, respectively). Idronoxil and paclitaxel given in combination (idronoxil 50 mg/kg p.o. once daily and paclitaxel 1 mg/kg i.p. q3d \times 4)

Table 1: Idronoxil augments the anticancer effect of different classes of cytotoxic drugs against a panel of cell lines representative of ovarian, pancreatic and prostate cancer.

Chemotoxic	Indication	Cell line	IC ₅₀ (μM)			Sensitization factor
			Idronoxil	Chemotoxic	Combined	
Cisplatin	Ovarian	A2780**	2.1	3	> 0.001 ^B	> 2000
		CP70**	3.8	10.6	1.5 ^B	7
		CP70***	"	"	0.12 ^B	88
	Pancreatic	HPAC*	32.1	49.6	7.7 ^D	6.4
Paclitaxel	Ovarian	A2780**	1.5	3.4 nM	0.033 nM ^B	104
		CP70**	37.5	1.7 nM	< 0.0001 nM ^B	> 2000
		SK-OV-3*	14.7	0.003	0.00014 ^C	25
	Prostate	PC-3**	87.5	0.05	1.30 ^E	> 2000
Gemcitabine	Ovarian	CP70**	2	0.4 nM	< 0.0001 nM ^B	> 2000
	Pancreatic	HPAC**	> 30	2.3	0.23 ^E	10
		HPAC*	> 30	3.7	0.03 ^E	150
Doxorubicin	Ovarian	CP70**	> 30	104 nM	0.002 nM ^D	> 2000
	Pancreatic	HPAC**	100	1.82	0.035 ^E	53
		HPAC*	11	0.033	3.2 ^E	> 2000
Camptothecin	Ovarian	A2780*	1	0.00027	2.64 ^E	103

*Combined; **idronoxil; ***chemotoxic; ^Aidronoxil 0.5 μM; ^Bidronoxil 2 μM; ^Cidronoxil 2.5 μM; ^Didronoxil 5 μM; ^Eidronoxil 10 μM.

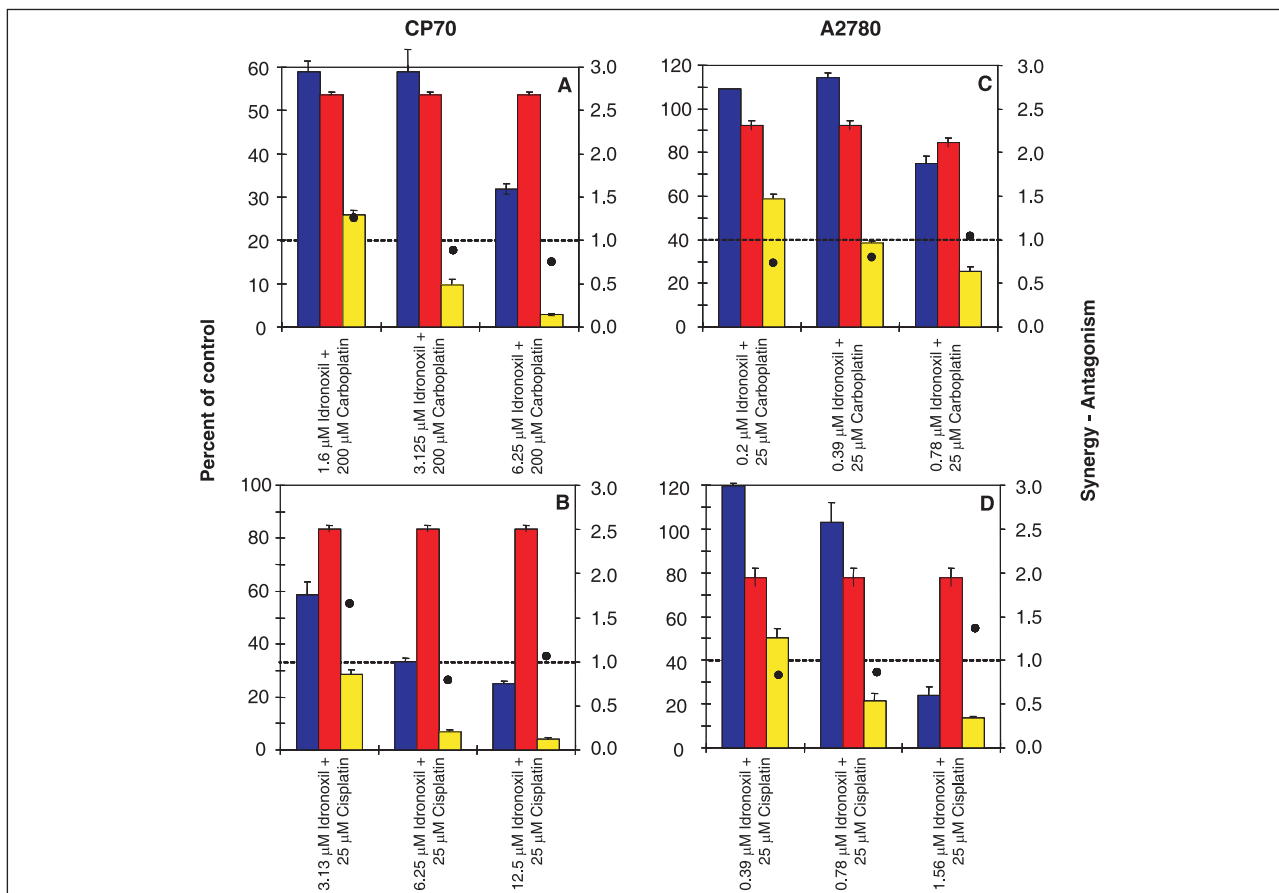


Fig. 1. Combination index analysis of synergistic toxicity against drug-sensitive (A2780) and -resistant (CP70) cell lines using idronoxil and two platinum drugs. Idronoxil–carboplatin (A) and idronoxil–cisplatin (B) combinations against platinum-resistant ovarian cancer cells (CP70) and idronoxil–carboplatin (C) and idronoxil–cisplatin (D) combination against platinum-susceptible ovarian cancer cells (A2780). Using combination index analysis any result below 1 (2nd Y-axis) is regarded as synergy. Blue column, idronoxil monotherapy control; red column, carboplatin monotherapy control; yellow column, idronoxil plus platinum; CI, analysis of synergy.

Table II: Idronoxil augments the anticancer effect of the platinum agents, paclitaxel, gemcitabine and topotecan in ovarian cancer xenograft models.

Tumor model	Dose and %T/C			Toxicity of combination compared to monotherapy controls
<i>Idronoxil (oral)–carboplatin (i.p.) - 1064-11-158</i>				
CP70	Idronoxil 50 mg/kg	Carboplatin 40 mg/kg	Idronoxil 25 mg/kg + carboplatin 20 mg/kg	Low-dose combination: no toxicity High-dose combination: marked weight loss Evidence of myelosuppression
%T/C	100	101	53.4*	Minor toxicity in kidney, spleen and colon by histology
<i>Idronoxil (oral)–cisplatin (i.p.) - 1064-11-158</i>				
CP70	Idronoxil 50 mg/kg	Cisplatin 4 mg/kg	Idronoxil 50 mg/kg + cisplatin 4 mg/kg	Low-dose combination: no augmented toxicity High-dose combination: severe weight loss Evidence of myelosuppression
%T/C	123.9	104.1	32.9*	Severe renal lesions by histology
<i>Idronoxil (i.p.)–cisplatin (s.c.) - 1063-1-12</i>				
A2780	Idronoxil 20 mg/kg	Cisplatin 1 mg/kg	Idronoxil 10 mg/kg + cisplatin 0.5 mg/kg	Low-dose combination: no augmented toxicity High-dose combination: no augmented toxicity
%T/C	29.2	31.8	17.4*	
<i>Idronoxil (oral)–gemcitabine (i.p.) - 1064-2-33</i>				
CP70	Idronoxil 100 mg/kg	Gemcitabine 2 mg/kg	Idronoxil 50 mg/kg + gemcitabine 1 mg/kg	Low-dose combination: no augmented toxicity High-dose combination: no augmented toxicity
%T/C	87	20.3	12.8*	
<i>Idronoxil (oral)–paclitaxel (i.p.) - 1064-3-16</i>				
CP70	Idronoxil 50 mg/kg	Paclitaxel 2 mg/kg	Idronoxil 50 mg/kg + paclitaxel 1 mg/kg	Low-dose combination: no augmented toxicity High-dose combination: no augmented toxicity
%T/C	70.7	38.1	38.5*	
<i>Idronoxil–topotecan - 1064-10-73</i>				
A2780	Idronoxil 25 mg/kg	Topotecan 2 mg/kg	Idronoxil 12.5 mg/kg + topotecan 1 mg/kg	Low-dose combination: mild weight loss High-dose combination: marked weight loss Evidence of myelosuppression; elevated ALP
%T/C	45.7	17	14.2	Minor toxicity in kidney, spleen and colon by histology

* $P < 0.05$

significantly retarded CP70 tumor xenograft growth at a level exceeding that observed in animals dosed with paclitaxel (2 mg/kg) or idronoxil (50 mg/kg) alone using the same route of administration and regimen (%T/C = 38.5 vs. 38.1 and 70.7, respectively). Idronoxil and topotecan dosed in combination (idronoxil 12.5 mg/kg p.o. and topotecan 0.1 mg/kg i.p. once daily \times 5) significantly retarded CP70 tumor xenograft growth at a level exceeding that observed in animals dosed with topotecan (2 mg/kg) or idronoxil (50 mg/kg) as monotherapy using the same route of administration and regimen (%T/C = 14.2 vs. 17 and 45.7, respectively).

A further study was conducted in athymic mice comparing the efficacy of idronoxil as a sensitizer of platinum-resistant ovarian cancer xenografts (CP70) to either cisplatin or carboplatin. Results indicated that while neither idronoxil nor platinum alone reduced terminal tumor weight, the same or reduced monotherapy doses when administered in combination led to significant reductions

in terminal tumor weights and overall tumor proliferation using both platinum drugs (Table II). These data confirm that idronoxil synergistically enhances the anticancer activity of a panel of cytotoxic agents with different modes of action against ovarian cancer xenografts.

The development of chemoresistance is a major hurdle in the effective short- to midterm treatment of cancer. There are diverse molecular events that contribute to the development of chemoresistant disease and it is thought that dysregulated expression of key players in the apoptotic cascade, through which many cytotoxic drugs act, is likely to contribute to the onset of chemoresistance. In ovarian cancer, intracellular blockers of caspase activity such as FLIP and XIAP are known to be overexpressed and contribute to chemoresistant disease. Apart from contributing to the stabilization of XIAP, overexpression of Akt has been shown to inhibit proapoptotic BAX and caspase-9 by phosphorylation, thereby serving to further uncouple the apoptotic cascade and facilitate the onset of

cells that are resistant to cytotoxic drugs. These events are orchestrated by intracellular ratios of ceramide and S1P, the balance of which can dictate cell death or survival. S1P has been shown to activate the Akt survival pathway which is known to be overexpressed in chemoresistant ovarian cancer (27-30).

Idronoxil disrupts intracellular ceramide:S1P stoichiometry due to its inhibitory effect on SK, leading to increased concentrations of ceramide and reduced concentrations of S1P. Increased intracellular ceramide results in caspase-2 activation, which in turn activates caspase-8 and regulators of mitochondrial integrity such as t-BID. Akt stabilization by S1P prosurvival pathways is also disrupted due to reduced intracellular S1P levels, resulting in activation of BAX and caspase-9. Reduced Akt expression also results in XIAP ubiquitination and degradation by the proteasome. Contributing to XIAP degradation is the release of Smac/Diablo and OMI/HtrA2. Hence, in concert, increased levels of caspase-2 activity, Akt degradation, XIAP removal, BAX and BID mobilization induced by idronoxil all contribute to the reactivation of the apoptotic cascade. Also contributing to the reactivation of apoptosis is the idronoxil-mediated degradation of FLIP, which re-engages death receptor-mediated apoptosis via caspase-8, thereby contributing to platinum resensitization. In concert, these mechanisms render the once drug-resistant cells sensitive to the death signals of cytotoxic drugs and explain idronoxil-induced chemosensitization (7, 8, 18, 20, 23, 31).

Pharmacokinetics and Metabolism

The pharmacokinetics of orally administered idronoxil were assessed in Sprague Dawley rats following bolus-dose nonlabeled and [^{14}C]-labeled idronoxil formulated in 1% carboxymethylcellulose (CMC). In the nonradiolabeled study, idronoxil was rapidly absorbed, with the t_{max} correlating with the first sample time point (Table III). Idronoxil was then rapidly eliminated from the plasma in a biphasic manner. A mean half-life for nonlabeled idronoxil of 6.59 h was derived from the elimination phase using

a noncompartmental model. The mean maximum concentration attained was 1.08 $\mu\text{g}/\text{ml}$ and the mean $\text{AUC}_{0-24\text{h}}$ value was 3.10 $\mu\text{g}\cdot\text{h}/\text{ml}$. These data indicate that idronoxil is orally bioavailable and that the parent drug has a relatively short half-life in this species.

In a pharmacokinetic study employing orally delivered [^{14}C]-idronoxil in both male and female Sprague Dawley rats, radioactivity was detected in plasma at the first sampling time point, indicating rapid absorption of the radiolabel from the stomach (Table IV). t_{max} values were highly variable in both male and female animals (0.25-8 h). Mean peak plasma concentrations were some 3-fold lower in females ($C_{\text{max}} = 4.17 \text{ mg eq}/\text{ml}$) compared to males ($C_{\text{max}} = 12.52 \text{ mg eq}/\text{ml}$) and the elimination half-life of the radiolabel was between 9 and 10 h for both sexes. Comparison of mean $\text{AUC}_{0-48\text{h}}$ values revealed that males have about 4-fold greater exposure to the label than females. Comparing absorption data from this oral study with a corresponding i.v. study (data not shown), it was apparent that the majority of the label was absorbed systemically after oral administration (females 95%, males 97%).

The tissue distribution of [^{14}C]-idronoxil was assessed in male albino Sprague Dawley rats by quantitative whole-body autoradiography following oral administration. Mean total radioactivity in various organs of albino rats at designated time points is reported in Table V. At 2 h postadministration, radioactivity was concentrated in the blood (5.8 $\mu\text{g eq}/\text{g}$), kidney cortex (7.5 $\mu\text{g eq}/\text{g}$) and whole kidney (7.1 $\mu\text{g eq}/\text{g}$), with the highest concentration found in the liver (9.2 $\mu\text{g eq}/\text{g}$). Remaining tissues had a radiolabel content of between 0.2 and 4.7 $\mu\text{g eq}/\text{g}$. At 8 h postadministration, the radiolabel content in most tissues had increased from levels observed at 2 h. Radioactivity was most prevalent in the blood (6.2 $\mu\text{g eq}/\text{g}$), kidney cortex (9.5 $\mu\text{g eq}/\text{g}$), whole kidney (9.5 $\mu\text{g eq}/\text{g}$), liver (10.7 $\mu\text{g eq}/\text{g}$) and nonsecretory component of the stomach (19.9 $\mu\text{g eq}/\text{g}$). Remaining tissues had concentrations of < 5.5 $\mu\text{g eq}/\text{g}$. Low levels were recorded in the brain and spinal cord (both below the limit of reliable measurement) and in the eye (0.908 $\mu\text{g eq}/\text{g}$ by LSC). Concentrations of

Table III: Mean model-independent plasma pharmacokinetic parameters for free (unconjugated) idronoxil after oral administration (40 mg/kg in 1% CMC) to male Wistar rats.

Gender (N)	Route	C_{max} ($\mu\text{g}/\text{ml}$)	t_{max} (h)	k_{el} (h^{-1})	$t_{1/2}$ (h)	$\text{AUC}_{0-24\text{h}}$ ($\mu\text{g}\cdot\text{h}/\text{ml}$)
Male (6)	p.o.	1.07 ± 0.47	0.60 ± 0.30	0.12 ± 0.02	6.59 ± 1.37	3.10 ± 0.93

Pharmacokinetic parameters were calculated for each animal and mean values were calculated for the group \pm SEM.

Table IV: Model-independent pharmacokinetic parameters for [^{14}C]-idronoxil in male and female rats following bolus oral and i.v. doses at a target dose of 20 mg/kg.

Gender (n)	Route	C_{max} ($\mu\text{g eq}/\text{ml}$)	t_{max} (h)	$t_{1/2\beta}$ (h)	$\text{AUC}_{0-48\text{h}}$ ($\mu\text{g eq}\cdot\text{h}/\text{ml}$)	Absorption (%)
Male (3)	p.o.	12.52 ± 6.80	3.42 ± 4.06	10.29 ± 2.98	200.46 ± 114.16	96
Female (3)	p.o.	4.17 ± 0.64	3.42 ± 4.06	12.56 ± 3.48	54.25 ± 22.35	100

Pharmacokinetic parameters were calculated for each rat and mean values were calculated for each subject group \pm SD.

Table V: Mean total radioactivity in the tissues of male albino rats after a single oral dose of [^{14}C]-idronoxil at a target dose of 20 mg/kg.

Tissue	Concentration ($\mu\text{g eq/g}$)				
	2 h	8 h	24 h	72 h	168 h
Adrenal cortex	2.1	2.2	0.7	NC	NC
Adrenal medulla	2.7	3.4	0.9	NC	NC
Adrenal (whole)	2.0	2.5	0.7	NC	NC
Bladder	1.7	2.9	1.2	NC	NC
Blood	5.8	6.2	1.2	NC	NC
Bone marrow	0.5	0.7	NC	NC	NC
Brain	*0.1	*0.1	*0.0	NC	NC
Brown fat	1.4	1.9	NC	NC	NC
Epididymis	1.0	1.9	0.9	NC	NC
Eye	0.2	0.3	*0.1	NC	NC
Harderian gland	0.9	1.5	0.7	NC	NC
Heart	1.6	1.9	0.5	NC	NC
Kidney cortex	7.5	9.5	5.2	1.0	0.3
Kidney medulla	4.0	4.4	1.7	*0.1	*0.0
Kidney (whole)	7.1	9.5	5.0	0.8	0.2
Lachrymal gland	0.9	1.7	0.3	NC	NC
Large intestine wall	1.1	5.3	NC	NC	NC
Liver	9.2	10.7	1.8	0.2	*0.0
Lung	4.7	5.5	1.2	NC	NC
Lymph node	0.8	0.9	0.3	NC	NC
Pancreas	1.6	1.5	NC	NC	NC
Pineal body	1.1	0.8	NC	NC	NC
Pituitary gland	1.2	1.8	0.5	NC	NC
Preputial gland	0.5	1.1	0.6	NC	NC
Prostate	0.7	1.2	NC	NC	NC
Rectum	0.9	1.5	2.0	NC	NC
Salivary gland	1.1	1.3	0.5	NC	NC
Seminal vesicles	0.3	0.3	NC	NC	NC
Skeletal muscle	0.4	0.5	NC	NC	NC
Skin - albino	1.1	1.8	0.8	NC	NC
Small intestine wall	2.9	5.2	NC	NC	NC
Spinal cord	*0.1	*0.1	NC	NC	NC
Spleen	0.7	0.7	0.4	NC	NC
Stomach wall (nonsecretory)	3.4	19.9	34.1	21.9	NC
Stomach wall (secretory)	1.9	1.8	0.8	NC	NC
Testes	0.7	0.9	0.3	NC	NC
Thymus	0.5	0.6	0.3	NC	NC
Thyroid gland	1.4	2.0	0.6	NC	NC
Uveal	0.6	0.7	0.4	NC	NC
White fat	0.2	0.2	NC	NC	NC
Right eye (LSC)	0.684	0.908	0.226	0.015	0.004

n = 3 animals/time point. *Below the limit of reliable measurement (0.1 $\mu\text{g eq/g}$). NP, not present; ND, not discernible; NC, not calculable; LSC, liquid scintillation counting.

the radiolabel in the nonsecretory portion of the stomach peaked at 24 h (34.1 $\mu\text{g eq/g}$), while at this time all other organs had markedly lower levels of the radiolabel. Significant levels of radioactivity were still noted in the kidney cortex (5.2 $\mu\text{g eq/g}$) and whole kidney (5.0 $\mu\text{g eq/g}$). At 72 h postadministration, high levels of radioactivity were still detected in the nonsecretory portion of the stomach (21.9 $\mu\text{g eq/g}$), while in other tissues no detectable radioactivity was present. By 168 h, radioactivity was virtually cleared from all tissues.

These data demonstrate that oral administration of [^{14}C]-idronoxil results in radioactivity being distributed at variable levels in most tissues of male rats, peaking 8 h postdose in the majority of tissues. The nonsecretory portion of the stomach showed the highest levels of radioactivity in the organs examined, peaking 24 h postdose. Significant levels of radioactivity were observed in the kidney and liver, indicating that idronoxil is subject to both

biliary and renal excretion. Little or no radioactivity was detected in the spinal cord or brain, suggesting that idronoxil is unable to cross the intact blood-brain barrier.

The excretion of [^{14}C]-idronoxil in the urine, feces and expired air was assessed in rats after oral administration. A large percentage of radiolabel was recovered in the feces (84.8% in males and 96.0% in females), with the majority of radioactivity excreted in the first 72 h (Table VI). In contrast, only a small proportion of radioactivity was recovered in the urine at 168 h (16.3% in males and 7.7% in females). Urinary excretion of the radiolabel appeared to be complete 24 h postadministration in both sexes. Less than 1% of the radiolabel was recovered in the cage wash and very low levels were recovered as expired air, in the gastrointestinal tract and the carcass. At the end of the sampling period, all administered radioactivity was accounted for in the tissues and matrices analyzed (102.3% in males and 104.8% in females).

Table VI: Percentage of administered dose collected in excreta following single doses of [^{14}C]-idronoxil to male and female mice.

	Time point	20 mg/kg p.o.	
		Male	Female
Urine	6	2.59	2.54
	24	13.14	6.55
	48	15.65	7.41
	168	16.32	7.65
Feces	24	69.02	75.67
	48	82.16	94.37
	72	84.19	95.61
	168	84.84	96.02
Cage wash		0.97	1.0
Gastrointestinal tract		0.01	0.013
Carcass		0.15	0.143
Total recovery		102.3	104.8

Values are mean cumulative percentages of the administered dose (3 rats/sex).

Table VII: Clinical pharmacokinetic parameters for conjugated idronoxil after a single oral dose of 400 mg in 9 patients.

	C_{\max} (ng/ml)	t_{\max} (h)	AUC _{0-6h} (ng.h/ml)
Mean	9590.12	3.28	38,872.75
SEM	2447.35	0.55	9357.14
Maximum	5946.32	1.50	20,909.65
Minimum	28,751.97	6.00	111,783.17

Plasma was collected over a 6-h period.

In humans, idronoxil has a low absolute oral bioavailability ($1.24 \pm 0.37\%$), although the bioavailability of conjugated idronoxil is much greater ($69.14 \pm 4.65\%$). Single- and repeated-dose pharmacokinetics of oral idronoxil were evaluated in male prostate cancer patients in trial NV06-0025. Conjugated and unconjugated idronoxil appeared in the plasma within 30 min of administration in most patients (unconjugated data not shown). On average, peak levels of conjugated idronoxil occurred between 2 and 3 h (Table VII). These data suggest that the drug is absorbed in the stomach and upper small intestine. Levels of free idronoxil were not consistently above the lower limit of quantitation for the assay (2.5 ng/ml), and as such, reliable pharmacokinetic parameter estimates could not be made. Steady-state concentrations of conjugated idronoxil were reached within 48 h following continuous 8-hourly dosing of 400 mg (Fig. 2). In these patients, concentrations at steady state varied between 10 and 70 $\mu\text{g/ml}$. These data indicate that steady-state plasma levels were rapidly attained and there was some degree of drug accumulation compared to single oral bolus dosing.

The nature and identity of metabolites of idronoxil were investigated in rats following oral administration of [^{14}C]-idronoxil. Organic solvent extracts of plasma, urine and feces samples were subject to radio-HPLC and LC-MS/MS analysis. In plasma, a single major radiation peak was identified as a monoglucuronide conjugate of idronoxil (VI) (Fig. 3). This component accounted for 11.618 and 1.161 $\mu\text{g eq/g}$ in plasma from male and female rats, respectively, 2 h following administration. The

major radiolabeled component present in male urine was identified as parent compound, accounting for 8.13% of the dose. Additional radiolabeled components were detected and identified as a ring-opened idronoxil (VII) and the monoglucuronide conjugate of idronoxil (VI), representing 2.04% and 2.89% of the administered dose, respectively. The radioactive profile for female rat urine following oral administration of radiolabeled idronoxil was different from that of male rats. No unchanged idronoxil was detected and the major radiolabeled component was a glucuronide conjugate of idronoxil (VI), which accounted for 4.04% of the administered dose. A further minor radiolabeled component was identified as a monoglucuronide conjugate of equol (VIII), the reduced form of idronoxil, accounting for < 1% of the administered dose. The radioactivity profiles in male and female feces following oral administration of [^{14}C]-idronoxil were qualitatively and quantitatively similar. The major component detected was identified as the parent compound and accounted for 31-35% of the administered dose in both sexes. The next most significant metabolite was a hydroxylated idronoxil (IX), accounting for about 28% of the administered dose in both male and female samples. A more polar peak identified as a dihydroxyidronoxil metabolite (X) was detected in both male and female feces, accounting for about 6.5% of the administered dose. An additional radiolabeled component was identified in female feces as an acetylhydroxyidronoxil metabolite (XI), accounting for 1.33% of the administered dose. The metabolic profile in urine from male rats following oral doses was considerably different from that in females. The major radiolabeled

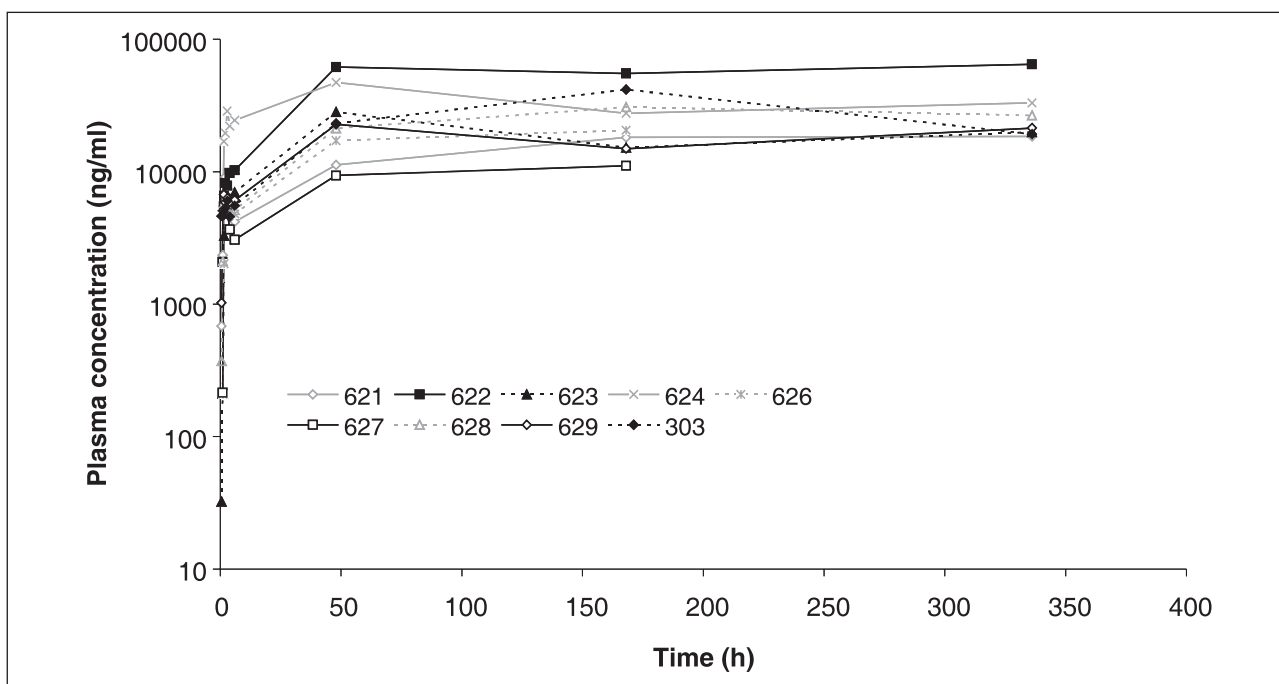


Fig. 2. Plasma concentration–time curves for conjugated idronoxil from 9 patients over 21 days during a regimen of idronoxil 400 mg t.i.d. Individual patient numbers provided in the box.

components detected in urine were identified as unchanged drug, ring-opened idronoxil (VII) and glucuronide conjugates of idronoxil (VI) and equol (VIII). The metabolic profile of feces from male and female rats after both dose routes was similar. The major radiolabeled components were identified as unchanged drug, hydroxyidronoxil (IX), dihydroxyidronoxil (X) and acetylhydroxyidronoxil (XI). The metabolic profile in plasma from both male and female rats consisted of only a glucuronide conjugate of idronoxil. It is postulated that biotransformation of idronoxil occurs through hydroxylation, acetylation and ring opening. Glucuronide conjugates of idronoxil and equol were also detected. These biotransformation routes are not unusual for a phenolic compound.

Safety

The potential of idronoxil to induce genetic mutations and chromosomal changes was assessed in the bacterial reverse mutation assay (Ames test) using five *Salmonella typhimurium* strains (TA98, TA100, TA102, TA1535 and TA1537) and an erythrocyte micronucleus test after oral administration of idronoxil in the Arc(S) mouse. The Ames test assesses the potential of a chemical entity to induce reverse mutations at the histidine locus in the genome of *S. typhimurium* in the presence and absence of a metabolic activation system (mammalian microsomal enzymes, S9 mix). This procedure is used to identify agents capable of inducing either base pair substitutions or frameshift mutations, which have implications for carcinogenicity. Idronoxil did not induce a threshold increase (a 2-fold increase for TA98, TA100

and TA102 and a 3-fold increase for TA1535 and TA1537) in the mean revertants per plate of at least one respective test strain over the mean revertants per plate of the appropriate vehicle control in either the initial or repeat assays. Accordingly, idronoxil was considered to be nonmutagenic under the assay conditions. The in vivo micronucleus test is designed to evaluate the potential of a chemical entity to induce micronuclei in the bone marrow of the specific pathogen-free Arc(S) (Swiss) mouse strain as a measure of damage to chromosomes (mitotic apparatus), and hence the assay is considered a measure of clastogenicity. Idronoxil was administered orally at a dose of 200 mg/kg in a 10% solution (w/w in 1% CMC). Mice were sacrificed 24, 48 and 72 h postadministration (n = 5 mice/sex). The polycyclic aromatic hydrocarbon 9,10-dimethyl-1,2-benzanthracene (DMBA) was used as the positive control. Idronoxil did not significantly increase the frequency of micronucleated polychromatic erythrocytes (MPCE) in any group of treated mice compared with the negative control group. Compared with negative control animals, DMBA treatment caused a significant increase ($P < 0.0001$) in the frequency of MPCE in both sexes at 48 h postadministration. These data demonstrate that idronoxil is nonclastogenic at the dose and time intervals evaluated under the criteria and experimental conditions of the protocol.

Idronoxil was found to be mutagenic in the in vitro mouse lymphoma thymidine kinase assay, where the mouse lymphoma L5178Y cell line was exposed to drug for 4 h and scored for forward mutations at the thymidine kinase locus ($tk^{+}tk^{-}$ to $tk^{-}tk^{-}$). Tests were conducted both in the absence and presence of a postmitochondrial

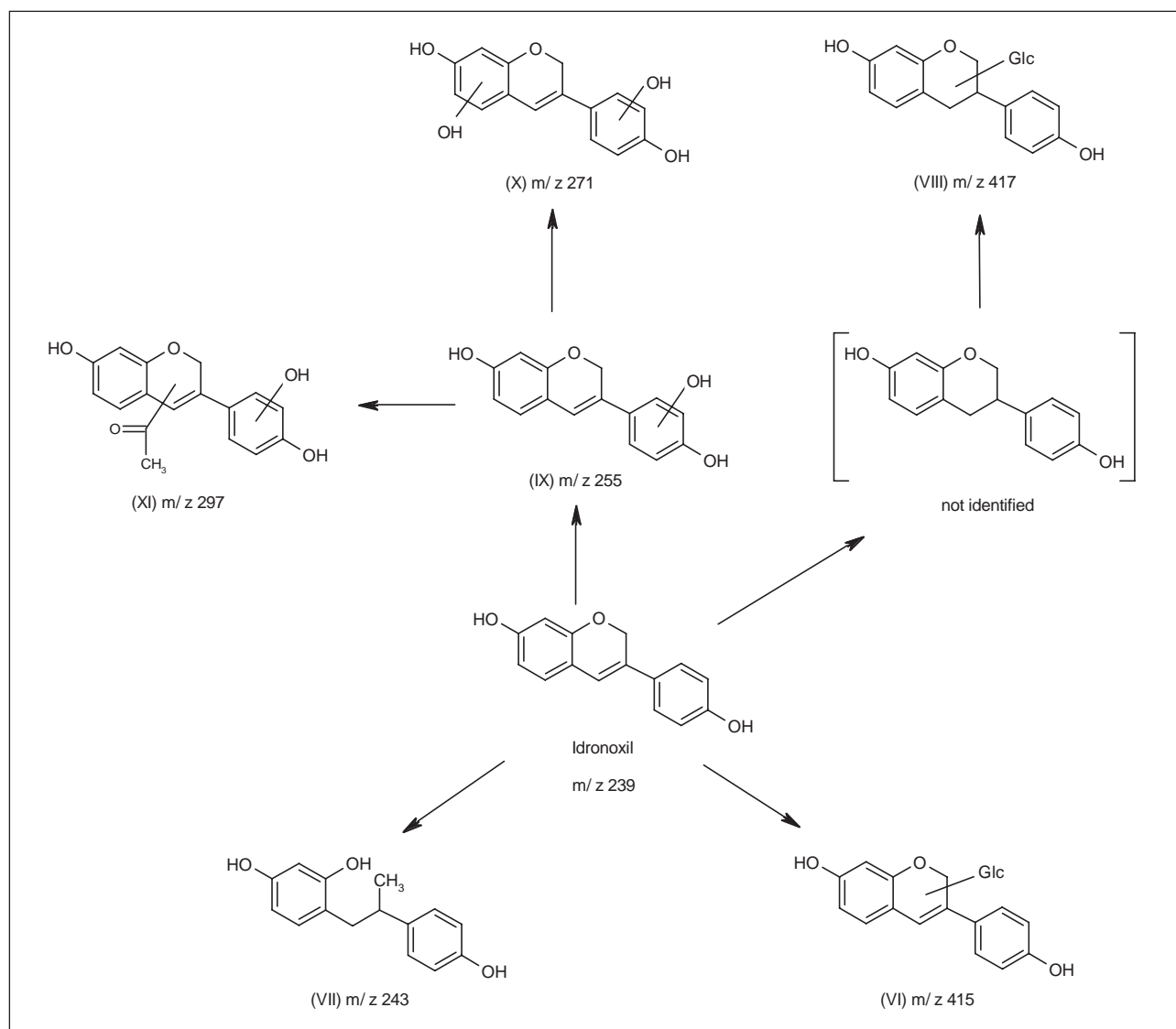


Fig. 3. Proposed biotransformation pathway of idronoxil. It is postulated that biotransformation occurs through hydroxylation, acetylation and ring opening. Glucuronide conjugates of idronoxil and equol were also detected.

supernatant fraction (S9 mix). Preliminary cytotoxicity tests showed that idronoxil was toxic to lymphoma cells at low concentrations, which is consistent with its broad anti-cancer activity. Idronoxil was shown to be mutagenic in the L5178Y cell line when tested at concentrations extending into the toxic range. The incidence of mutants above the accepted IWGT criterion for a biologically relevant increase in induced mutant fraction was observed at relatively nontoxic concentrations of idronoxil (2.5 µg/ml) in the presence of the S9 mix.

Idronoxil was administered daily over 49 days by oral gavage to 5 groups of 16 rats (8 animals per gender) at dose levels of 5, 15, 30, 80 and 150 mg/kg/day. A corresponding group of 16 rats (8 animals per gender) received vehicle only. Additional animals were included in vehicle control and high-dose (150 mg/kg/day) groups (5 animals per gender) to serve as recovery animals follow-

ing cessation of dosing to assess reversibility of any toxicity. A toxicokinetic analysis was also included as part of the study. No deaths were observed in any group. Moderately to severely increased water consumption was observed at 80 mg/kg, reaching significance at 150 mg/kg in both genders. In male rats, body weight gain was significantly reduced in the 80 and 150 mg/kg/day groups. In males, food intake was affected significantly in the 150 mg/kg/day group. In female rats, body weight gain was significantly reduced in the 80 mg/kg/day group. In treated females, statistically significantly lower food intake was seen from 30 mg/kg/day. Urea and creatinine elevations were observed at day 28 in females only. Blood analysis revealed drug-related changes in urea, creatinine, red cell parameters, white cell count, Europhile count, bilirubin, γ-glutamyltransferase and cholesterol in the 80 and 150 mg/kg/day groups of both genders, with

no obvious changes in the 5, 15 and 30 mg/kg/day groups. Urea and creatinine were elevated in the 150 mg/kg/day groups of both genders by the completion of the in-life phase (day 50), which is consistent with renal damage. In the recovery groups, changes were seen in urea, creatinine and hemoglobin. These changes were consistent with persistent (irreversible) renal damage. Histopathology analysis at day 50 showed that the two highest doses (80 and 150 mg/kg/day) were associated with renal damage (tubulointerstitial nephritis), with probable secondary thymic and splenic changes in the highest dose group. There were no obvious changes in the 5, 15 and 30 mg/kg/day groups. The level of free idronoxil in the plasma of females dosed at 5 mg/kg/day and all animals dosed at 15-150 mg/kg/day peaked between 0.5 and 4 h after dosing in week 1 and between 0.25 and 4 h after dosing in week 7. The level of total idronoxil in the plasma of the animals receiving 15-150 mg/kg/day peaked between 0.25 and 24 h after dosing in weeks 1 and 7. The plasma values for free idronoxil were much lower than for total idronoxil, suggesting that most of the circulating idronoxil was present in the conjugated form.

The maximum tolerated dose (MTD) of idronoxil was determined in beagle dogs after daily oral gavage. One male and one female beagle dog were assigned to an escalating-dose study and received idronoxil orally by gavage (1% CMC as vehicle) at escalating dose levels of 10, 50, 100, 200, 400, 800 and 1000 mg/kg/day for a 3- or 4-day period at each dose level. On all dosing occasions a constant dose volume of 5 ml/kg body weight was used. The only abnormal findings observed in the MTD study were feces of abnormal consistency in those animals receiving the highest dose (1000 mg/kg) about 2-6 h postadministration. Body weight and food consumption were unaffected by treatment, as were organ weights, and there were no treatment-related macroscopic findings.

In a repeated-dose study in two groups of 3 male and 3 female dogs, idronoxil was administered orally by gavage at fixed dose levels of 100 and 800 mg/kg/day for 28 days. Colored feces of abnormal consistency were observed in animals receiving the higher dose. There was also a low incidence of vomiting in female dogs receiving 800 mg/kg/day. Body weight and food consumption were unaffected by treatment. There were no ocular changes related to treatment. Toxicokinetic investigations following single doses of idronoxil 100 and 800 mg/kg/day revealed that systemic exposure to both free and total idronoxil (idronoxil plus conjugates) increased with increasing dose, generally with a less than proportional relationship to dose. However, exposure to free idronoxil was substantially lower than to total idronoxil and suggested that most of the circulating drug was present as either sulfate or glucuronide conjugates. Although mean estimates of $C_{\max(\text{obs})}$ generally increased following repeated dosing, there was no evidence to suggest that either total (idronoxil plus conjugates) or free idronoxil accumulated in animals at 100 or 800 mg/kg/day. Where estimated, terminal elimination half-lives ($t_{1/2}$) suggested that steady-state concentrations would be expected to be

reached after approximately 2 days for free idronoxil and 3 days for idronoxil plus conjugates, and as such, data from day 28 of this study could be considered to represent steady-state conditions. There were no consistent or appreciable gender-related differences in any of the toxicokinetic parameters reported in this study. There were no treatment-related hematological findings or plasma biochemical findings and no changes in urinary composition during week 4 of treatment. Organ weights were unaffected by treatment and there were no treatment-related macroscopic findings. Minimal to mild bile duct hyperplasia and pigment deposits in Kupffer cells in the liver were observed in males that received 800 mg/kg/day. It was concluded that oral administration of idronoxil at doses of up to 1000 mg/kg/day was associated with abnormally colored feces of abnormal consistency. During the 28-day repeated-dose phase at 800 mg/kg/day, abnormally colored and abnormal-consistency feces persisted and histopathological findings of bile duct hyperplasia and pigment deposits in Kupffer cells were present in the liver of males. Systemic exposure to idronoxil increased less than proportionally to dose at up to 800 mg/kg/day. The dose of 800 mg/kg/day was considered to be the MTD and would be considered suitable for repeated-dose administration in this species.

As part of the dog study, electrocardiograms were taken on day 2 and during week 4 of Part B before dosing and at 2 h after dosing. Electrocardiograms were recorded for the standard limb lead (lead II) and the signals obtained from lead II were evaluated and the interval data (P-R, QRS and Q-T waves) and heart rate derived. In addition, the R-R interval was determined from the heart rate to calculate the $Q-T_c$ interval using Van de Water's and Fridericia's formulas. The data demonstrated no abnormalities in the electrocardiogram analysis, suggesting that idronoxil is not associated with cardiac repolarization toxicity. These data are consistent with the results from a functional human ether-a-go-go-related gene (hERG) binding assay. The hERG potassium ion channel conducts rapidly activating delayed rectifier K^+ currents (K_{ir}) that critically contribute to cardiac repolarization. Drug-induced blockade of K_{ir} currents has been linked to delayed repolarization of action potentials, resulting in a prolonged Q-T interval (32). The potential of idronoxil to disrupt the ventricular action potential and induce Q-T prolongation was assessed using a competitive hERG radioligand binding assay. Idronoxil (10 μM) did not inhibit hERG activity.

Clinical Studies

An i.v. dosage formulation of idronoxil has been evaluated for safety, tolerability and efficacy as monotherapy in solid tumors in five clinical studies.

Two phase Ia studies have been completed. The first study was conducted in 6 patients (3 males and 3 females aged 51-75 years) with metastatic breast or prostate cancer. Idronoxil was infused at a dose of 5 mg/kg at a rate of 1 ml/min over approximately 5 min using a standard

infusion pump. Plasma was collected at regular intervals up to 8 h postinjection. The levels of free (unconjugated) idronoxil and total (free + conjugated) idronoxil were determined by HPLC. The maximum concentration (C_{max}), the time to maximum concentration (t_{max}), the area under the plasma concentration–time curve (AUC) and the terminal plasma elimination half-life ($t_{1/2}$) were calculated using a standard pharmacokinetic program. Idronoxil was well tolerated by all patients. The only side effects were transient mild flushing and nausea in 4 of the 6 patients during the immediate infusion period. The remaining 2 patients were treated with antihistamine (Phenergan) i.v. immediately prior to commencement of the infusion and did not report flushing or nausea. No significant changes in vital signs (body temperature, heart rate, blood pressure) occurred in any patient over the 8-h postinjection observation period. The mean $t_{1/2}$ of unconjugated idronoxil was relatively short, approximately 0.7 h, and longer (2.92 h) for conjugated idronoxil.

The second phase Ia study was conducted in 5 patients (3 males and 2 females) with metastatic cancer who were given idronoxil by continuous i.v. infusion for approximately 10 half-lives (5 h) at a dose of 1 mg/kg/h. This dose was calculated to deliver steady-state levels of free idronoxil in plasma between 0.6 and 1.0 $\mu\text{g/ml}$. No adverse effects were reported or observed for the duration of the infusion and for a period of 7 days postinfusion. No nausea was reported. One patient was infused for 3.5 h only. The other 4 patients received the full 5-h infusion. Steady-state levels of free (unconjugated) idronoxil in the range of 0.6–1.1 $\mu\text{g/ml}$ were achieved.

A phase Ib study involved 21 patients with solid malignancies who had become refractory to standard anticancer therapies. Idronoxil was administered by single weekly bolus injection for 12 consecutive weeks. The lowest dose was 1.3 mg/kg/dose and the highest dose was 30 mg/kg/dose. Results showed no drug-associated toxicity. There were two cases of hypersensitivity reactions (myalgia, fever), one of which was adequately managed by pre-treatment with antihistamines and an antinauseant; the second patient was withdrawn from the study. The main outcomes of that study can be summarized as follows. Five of 21 patients had grade 1 nausea that was managed with metoclopramide. Two of 21 patients had hypersensitivity reactions (flushing, back pain). One of these patients also had transient thrombocytopenia and was withdrawn from the study. The other patient was adequately managed with steroid and antihistamine premedication; no other toxicities were encountered and the MTD was not reached. Fourteen of 21 patients experienced disease progression and were withdrawn from the study prior to completion. Seven of 21 patients were able to complete 12 weeks of treatment without disease progression and 2 of these (renal carcinoma, pancreatic carcinoma) completed 18 weeks of treatment without disease progression.

Study NV06-0023 (phase Ib) involved 21 patients with solid malignancies who had failed standard anticancer therapy. Idronoxil was administered by continuous i.v. infusion over a minimum of 3 treatment cycles, with each

treatment cycle comprising 7 days of infusion followed by 7 days with no infusion. The lowest dose was 1.3 mg/kg/24 h and the highest dose was 40 mg/kg/24 h. No drug-related toxicities were encountered and the MTD was not reached; no intolerance was reported. No objective tumor responses were obtained although 3 of 21 patients were able to continue therapy beyond 3 treatment cycles with stable disease.

Study NV06-0024 (phase Ib) included 19 patients with solid malignancies who had failed standard anticancer therapies. Idronoxil was administered by continuous i.v. infusion over a minimum of 3 treatment cycles, with each treatment cycle comprising 7 days of infusion followed by 7 days with no infusion. The lowest dose was 0.32 mg/kg/24 h and the highest dose was 47 mg/kg/24 h (33). No drug-related toxicities were encountered and the MTD was not reached; no intolerance was reported. Seven of 19 patients were withdrawn before the conclusion of 3 treatment cycles due to disease progression; 4 of 19 were evaluated as having disease stabilization after 3 treatment cycles and were able to continue therapy.

The objective of study NV06-0029, a phase Ib study, was to determine whether idronoxil monotherapy had an antitumor effect and to identify appropriate doses for a planned follow-on combination therapy study. The study was conducted in patients with advanced ovarian cancer who had failed at least two lines of standard chemotherapy. Patients were treated at one of four dose levels (1, 3, 10 or 20 mg/kg i.v.; 10 patients per dose). A bolus infusion of idronoxil was administered weekly on 2 consecutive days over 10–20 min. Treatment cycles were of 12 weeks' duration. Toxicity was scored according to NCI criteria. Responses were defined according to RECIST criteria in patients with measurable disease or Rustin criteria in evaluable patients with CA125 criteria. Treatment was continued until patients showed disease progression; response to therapy was assessed by blood levels of CA125, shrinkage of the tumor mass or improved clinical status. The best response was stable disease (RECIST criteria) in 4 of 41 (10%) women at 3 months, and no objective evidence of tumor shrinkage (defined as complete or partial response by RECIST criteria) was observed, although 1 platinum/paclitaxel-refractory patient remained progression-free for 36 weeks. However, 10 (25%) of the 40 patients had responded when assessed after 6 weeks of treatment, although tumor mass was not assessed at this time. In 6 of these patients, CA125 levels had fallen by an average of 54%; in the other 4 patients, rapidly rising CA125 levels before the trial commenced had stopped rising (stabilization) at 6 weeks. At 3 months, 4 of these 10 patients showed stabilized CA125 levels. Almost all of these responders were in the two lowest dose groups, confirming laboratory studies that showed a greater antitumor effect at lower doses for idronoxil. No toxicities were noted. To explore a possible role for idronoxil as a chemosensitizing agent for late-stage cancers, following completion of the idronoxil therapy, a number of the patients were rechallenged with standard chemotoxic drugs. In 10 patients who received

Table VIII: Tumor response data for subjects in groups 1 and 2 of study NV06-0037.

Best response (RECIST)	Cisplatin + idronoxil	Paclitaxel + idronoxil
No. patients	21	19
CR	0	1
PR	6	2
Objective response rate	29%	16%
SD	9	11
PD	6	5
Disease control rate	71%	74%

CR, complete response; PR, partial response; SD, stable disease; PD, progressive disease.

paclitaxel, 8 responded with an immediate and marked decline (average 64%) in CA125 levels; the other 2 women failed to respond and showed progressive disease. Five of the 10 women treated with paclitaxel were previously considered either resistant or refractory to paclitaxel. However, after treatment with idronoxil and subsequent treatment with paclitaxel, 4 of these 5 patients showed a marked response in their CA125 levels and 3 remained alive after an average of 292 days.

Study NV06-0037 (phase II) was a 5-arm, open-label efficacy and safety study conducted in women with recurrent ovarian, fallopian and primary peritoneal cancer. Patients had cancer that was resistant (disease progression within 6 months) or refractory (disease progression while on therapy) to platinum agents or taxanes. Only the i.v. dosage form of idronoxil was used in this study, and it was administered on 2 consecutive days per week (3 mg/kg) with either paclitaxel (80 mg/m²) or cisplatin (40 mg/m²) dosed weekly immediately following and on the same day as the second weekly idronoxil injection. Treatment cycles were 6 weeks in duration and treatment continued for 8 cycles unless there was disease progression or dose-limiting toxicity. The primary objectives of the study were: 1) to measure the safety of combination therapy with idronoxil and cisplatin or paclitaxel; and 2) to determine the relative efficacy of idronoxil in the reversal of platinum- and taxane-based chemoresistance. There were 5 treatment groups. Group 1 (19 subjects) had tumors that were resistant or refractory to platinum drugs (disease relapse within 6 months of therapy). They were treated on enrollment with a combination of i.v. idronoxil + cisplatin. Group 2 consisted of 21 subjects with tumors that were resistant or refractory to taxane drugs. They were also treated with a combination of i.v. idronoxil + paclitaxel. Group 3 (10 subjects) had tumors that were resistant or refractory to taxane drugs and they were given a paclitaxel run-in (weekly therapy). During the run-in phase, they were administered the combination drug, either paclitaxel (in this instance) or carboplatin (as described in treatment groups 4 and 5 immediately below), until they experienced disease progression, at which time idronoxil treatment was begun in association with the combination drug. Those patients showing disease progression (> 25% increase in CA125 levels) within 12 weeks were treated with i.v.

idronoxil + weekly paclitaxel. Group 4 consisted of 10 subjects with tumors that were resistant or refractory to platinum drugs who were given a carboplatin run-in (weekly therapy). Those patients showing disease within 12 weeks were treated with i.v. idronoxil + weekly carboplatin. Group 5 (10 subjects) had tumors that were resistant or refractory to platinum drugs and were given a carboplatin run-in (weekly therapy). Those patients showing disease progression within 12 weeks were treated with oral idronoxil + weekly carboplatin. The results for patients recruited to groups 1 and 2 were reported at the 2006 Annual Meeting on Women's Cancer (March 22-26, Palm Springs). The data are shown in Table VIII. The disease control rate, or the sum of complete responses (CR) + partial responses (PR) + stable disease (SD) as a percentage of the total, can be calculated from these data as 71% for idronoxil + cisplatin and 74% for idronoxil + paclitaxel. This is a measure of the proportion of women who had not progressed, i.e., who were "progression-free". Progression-free survival (PFS) is now a recognized surrogate endpoint and accepted by the FDA in place of the objective response rate. While the numbers of women who were "progression-free" were recorded in this study, the duration (i.e., PFS) was not determined. However, as a post-study exercise, median overall survival was observed to be 62 weeks for the idronoxil + cisplatin arm and 48 weeks for the idronoxil + paclitaxel arm compared to a published median survival reported for patients on standard therapy of only 28-40 weeks (34). It seems likely therefore that the PFS in this study would have been substantially improved by idronoxil therapy. No limitation was imposed at the time of enrollment on the length of time between completion of the prior course of chemotherapy and commencement of combination therapy.

In light of other studies that have shown that an elapsed time of 12 months from the completion of a course of chemotherapy is a critical time in terms of restoration of chemosensitivity (35), in the current phase III OVATURE (OVarian Tumor REsponse) protocol, eligibility is restricted to women who progressed on platinum therapy no more than 6 months prior to entry. This stringency has been introduced to ensure that there is little likelihood of spontaneous resensitization to platinum, which may occur over longer time frames. Additional data

Table IX: Tumor response data for treatment group 1 in study NV06-0037 in subsets of patients either < 6 months or > 6 months since completion of the prior course of platinum.

Best response (RECIST)	< 6 months	> 6 months
No. patients	10	11
CR	0	1
PR	3	3
Objective response rate	30%	27%
SD	5	4
PD	2	4
Disease control rate	80%	64%

CR, complete response; PR, partial response; SD, stable disease; PD, progressive disease.

Table X: Prostate-specific antigen (PSA) responses in patients in study NV06-0025.

Dose (mg/day)	n	PSA response	PSA doubling time (weeks)	Time to progression (weeks)
20	6	0	14	35
80	6	0	22	58
200	5	1	66	70
400	9	2	39	86

from study NV06-0037, presented at the 2006 Society of Gynecologic Oncologists (SGO) meeting, confirm that this category of platinum-resistant women will be expected to show improved PFS on combination idronoxil + carboplatin therapy. Table IX shows a subset analysis of the tumor response data for 21 patients in the idronoxil + cisplatin group according to the time since last platinum therapy, i.e., either < 6 months or > 6 months since completion of the prior course of platinum chemotherapy. For patients in the high-stringency group (< 6 months), 80% were progression-free, which reinforces the expectation that a significant PFS will be achieved in the OVATURE protocol (see below).

The NV06-0025 study involved patients with late-stage, hormone-refractory prostate cancer. This was a multicenter trial conducted in Australia and the primary objectives were safety, tolerability and efficacy. The subjects were men with malignant prostate cancer and rising prostate-specific antigen (PSA) levels (mean 60 ng/ml at start of study) who had become unresponsive to antiandrogen therapy. These patients were treated with idronoxil capsules 3 times daily for 3 weeks each month up to a maximum of 6 months. A treatment cycle consisted of daily treatment for 21 consecutive days followed by 7 days with no treatment. Patients received one of four different doses: 20, 80, 200 or 400 mg t.i.d. There were 6 patients in the 20- and 80-mg groups, 5 in the 200-mg group and 9 in the 400-mg group. Toxicity was scored according to NCI criteria and responses were defined on the basis of PSA levels (disease status defined as "progressive" or "stabilized" relative to pretreatment levels) and clinical status. There were no toxicities related to idronoxil therapy in men treated for periods up to 40 weeks. Pharmacokinetic analysis revealed that idronoxil

was almost completely (> 99.5%) conjugated as glucuronide or sulfate salts in blood. The mean steady-state blood levels of conjugated idronoxil for the 20, 80, 200 and 400 mg/dose groups were 2.0, 7.3, 13.6 and 20.5 µg/ml, respectively. The results of efficacy evaluations at 3 months are shown in Table X. A total of 26 patients completed the study. Two of the 14 patients treated with the two highest doses showed a decline in PSA levels of > 50%. PSA doubling time increased a mean of 43 weeks from low-dose (control) patients to high-dose patients. Time to progression reflected a dose-dependent trend, being 35 weeks in the 20-mg group, 58 weeks in the 80-mg group, 70 weeks in the 200-mg group and 86 weeks in the 400-mg group.

Study NV06-0031 is being conducted in patients with squamous cell carcinoma and adenocarcinoma of the cervix, vagina and vulva. This is a neoadjuvant design study in which the subjects will receive 4 weeks of daily oral idronoxil treatment in the period between a primary diagnosis of cancer and scheduled surgical resection or radiotherapy. The study will evaluate the safety and ability of idronoxil to act as an effective anticancer agent when given as monotherapy in early-stage cancer. A total of 20 patients will be enrolled in the study. There are three dose groups: 50, 200 and 400 mg idronoxil given orally t.i.d. The primary endpoints will be tumor size and histological grading. Fourteen patients have completed treatment on either 50 mg (6 patients) or 200 mg (8 patients) without drug-associated toxicity or intolerance. Tumor response is being assessed over the 28-day treatment period both by a change in tumor burden (RECIST) and by histological evidence of a biological effect (e.g., apoptosis). No PRs by RECIST criteria (reduction in the sum longitudinal diameter of > 30%) have been observed to

Table XI: Effect of idronoxil on the catalytic activity of nine human cytochrome P-450 isoenzymes.

Cytochrome P-450 isoenzyme	Inhibitor/substrate	IC ₅₀
CYP1A2	Furafylline/CEC	> 333 μ M
CYP2A6	Tranylcypromine/coumarin	> 333 μ M
CYP2B6	Tranylcypromine/EFC	> 333 μ M
CYP2C8	Quercetin/DBF	66.0 μ M
CYP2C9	Sulfaphenazole/MFC	25.1 μ M ^a
CYP2C19	Tranylcypromine/CEC	67.1 μ M ^a
CYP2D6	Quinidine/AMMC	> 1000 μ M
CYP2E1	DDTC/MFC	> 1000 μ M
CYP3A4	Ketoconazole/BFC	24.3 μ M ^a
	Ketoconazole/BQ	> 111 μ M ^b

^a1000 μ M excluded from data analysis. ^b100 and 333 μ M excluded from data analysis. CEC, 3-cyano-7-ethoxycoumarin; EFC, 7-ethoxy-4-trifluoromethylcoumarin; DBF, dibenzylfluorescein; MFC, 7-methoxy-4-trifluoromethylcoumarin; AMMC, 3-[2-(*N,N*-diethyl-*N*-methylamino)ethyl]-7-methoxy-4-methylcoumarin; BFC, 7-benzoyloxy-4-(trifluoromethyl)coumarin; BQ, 7-benzoyloxyquinoline.

date, but of 6 patients treated with 50 mg, SD and disease progression (DP) were seen in 5 and 1, respectively; of 8 patients treated with the dose of 200 mg, all patients were classified as SD; enrollment in the 400-mg group has yet to be completed. This trend suggests an antitumor effect of idronoxil in this setting, which was supported by the histological evidence of an increase in the apoptotic index and a decrease in the mitotic index in the 200-mg group.

In view of the efficacy of idronoxil in chemosensitizing platinum-resistant patients in study NV06-0037, and the bioequivalence of idronoxil given by the oral route, a pivotal phase III study has now commenced. This study, known as the OVATURE study, is a multicenter, randomized, double-blind efficacy study comparing idronoxil (oral dosage form) in combination with carboplatin versus carboplatin with placebo in patients with platinum-resistant or -refractory late-stage epithelial ovarian, fallopian or primary peritoneal cancer following at least second-line platinum therapy. The OVATURE trial is a major phase III clinical trial to determine the safety and efficacy of idronoxil when used in combination with carboplatin. The OVATURE trial is recruiting ovarian cancer patients whose cancer initially responded to chemotherapy but has since become resistant or refractory to traditional platinum treatments. The OVATURE trial has been approved by the U.S. FDA under a Special Protocol Assessment (SPA) program. The primary endpoint of the trial is to compare the effect of each treatment regimen on PFS and the secondary endpoint is to compare the effect of each treatment regimen on overall survival. The protocol provides for an interim analysis of the data, which, if statistically significant, can be used to support a request for accelerated marketing approval. An analysis of interim results will be possible after the targeted patient recruitment to this study is completed and 95 events have been recorded, an event representing death or disease progression. Under the SPA-approved protocol for OVATURE, patients are to be enrolled and randomized to two treatment arms: carboplatin + idronoxil and carboplatin + placebo. Carboplatin will be administered i.v. weekly and idronoxil or placebo will be administered as capsules every 8 h on a continuous daily basis. The statistical plan indicates that, based on the assumptions of 8 months'

PFS in the treated group compared to 5 months' PFS in the control group, a total of 340 completed patients will be sufficient to demonstrate a statistically significant effect. The trial currently involves 70 sites in the U.S., the U.K., Europe and Australia.

Drug Interactions

In vitro, idronoxil has been shown to inhibit the catalytic activity of human cytochrome P-450 isozymes CYP2C8, CYP2C9, CYP2C19 and CYP3A4/BFC at physiologically relevant concentrations. The ability of idronoxil (0.457-3000 μ M) to inhibit a panel of nine human CYP isozymes (CYP1A2, CYP2A6, CYP2B6, CYP2C8, CYP2C9, CYP2C19, CYP2D6, CYP2E1, CYP3A4/BFC and CYP3A4/BQ) was tested in suspensions of microsomes. Idronoxil significantly inhibited the activity of CYP2C8, 2C9, 2C19 and 3A4/BFC isoforms and partially inhibited 1A2, 2A6, 2D6, 2E1 and 3A4/BQ (Table XI). The data suggest that drug interactions between idronoxil and coadministered drugs (or endogenous substrates) which are metabolized by these enzymes may potentially occur in the clinic.

Source

Marshall Edwards Inc.

References

1. Lambert, J.D., Hong, J., Yang, G.Y. et al. *Inhibition of carcinogenesis by polyphenols: Evidence from laboratory investigations*. Am J Clin Nutr 2005, 81(1, Suppl.): 284S-91S.
2. Williamson, G., Manach, C. *Bioavailability and bioefficacy of polyphenols in humans. II. Review of 93 intervention studies*. Am J Clin Nutr 2005, 81(1, Suppl.): 243S-55S.
3. Khan, N., Adhami, V.M., Mukhtar, H. *Apoptosis by dietary agents for prevention and treatment of cancer*. Biochem Pharmacol 2008, Epub ahead of print.
4. Meeran, S.M., Katiyar, S.K. *Cell cycle control as a basis for cancer chemoprevention through dietary agents*. Front Biosci 2008, 13: 2191-202.

5. Jänicke, R.U., Sohn, D., Schulze-Osthoff, K. *The dark side of a tumor suppressor: Antiapoptotic p53*. Cell Death Differ 2008, 15(6): 959-76.
6. Cuvillier, O. *Downregulating sphingosine kinase-1 for cancer therapy*. Expert Opin Ther Targets 2008, 2(8): 1009-20.
7. Alvero, A.B., Kelly, M., Rossi, P. *Anti-tumor activity of phenoxodiol: From bench to clinic*. Fut Oncol 2008, 4(4): 475-82.
8. Alvero, A.B., O'Malley, D., Brown, D. et al. *Molecular mechanism of phenoxodiol-induced apoptosis in ovarian carcinoma cells*. Cancer 2006, 106(3): 599-608.
9. Kamsteeg, M., Rutherford, T., Sapi, E. et al. *Phenoxodiol—an isoflavone analog—induces apoptosis in chemoresistant ovarian cancer cells*. Oncogene 2003, 22(17): 2611-20.
10. Kluger, H.M., McCarthy, M.M., Alvero, A.B. et al. *The X-linked inhibitor of apoptosis protein (XIAP) is up-regulated in metastatic melanoma, and XIAP cleavage by phenoxodiol is associated with carboplatin sensitization*. J Transl Med 2007, 5: 6-20.
11. Baudhuin, L.M., Cristina, K.L., Ju, J. et al. *Akt activation induced by lysophosphatidic acid and sphingosine-1-phosphate requires both mitogen-activated protein kinase kinase and p38 mitogen-activated protein kinase and is cell-line specific*. Mol Pharmacol 2002, 62(3): 660-71.
12. Kim, D.S., Hwang, E.S., Lee, J.E., Kim, S.Y., Park, K.C. *Sphingosine-1-phosphate promotes mouse melanocyte survival via ERK and Akt activation*. Cell Signal 2003, 15(10): 919-26.
13. Shida, D., Takabe, K., Kapitonov, D. et al. *Targeting Sp hK1 as a new strategy against cancer*. Curr Drug Targets 2008, 9(8): 662-73.
14. Kim, W.H., Kang, K.H., Kim, M.Y. et al. *Induction of p53-independent p21 during ceramide-induced G1 arrest in human hepatocarcinoma cells*. Biochem Cell Biol 2000, 78(2): 127-35.
15. Pettus, B.J., Chalfant, C.E., Hannun, Y.A. *Ceramide in apoptosis: An overview and current perspectives*. Biochim Biophys Acta 2002, 1585(2-3): 114-25.
16. Carpinteiro, A., Dumitru, C., Schenck, M., Gulbins, E. *Ceramide-induced cell death in malignant cells*. Cancer Lett 2008, 264(1): 1-10.
17. De Luca, T., Morre, D.M., Zhao, H. et al. *NAD⁺/NADH and/or CoQ/CoQH₂ ratios from plasma membrane electron transport may determine ceramide and sphingosine-1-phosphate levels accompanying G1 arrest and apoptosis*. Biofactors 2005, 25(1-4): 43-60.
18. Cabot, M.C., Yu, J.Y., Kelly, G.E. et al. *Phenoxodiol, a synthetic analog of genistein, generates ceramide and is equipotent in wild-type and multidrug-resistant human tumour cells*. 41st Annu Meet Am Soc Clin Oncol (ASCO) (May 13-17, Orlando) 2005, Abst 2075.
19. Gamble, J.R., Xia, P., Hahn, C.N. et al. *Phenoxodiol, an experimental anticancer drug, shows potent antiangiogenic properties in addition to its antitumour effects*. Int J Cancer 2006, 118(10): 2412-20.
20. Morre, D.J., Chueh, P.J., Yagiz, K. et al. *ECTO-NOX target for the anticancer isoflavone phenoxodiol*. Oncol Res 2007, 16(7): 299-312.
21. Brown, D.M., Kelly, G.E., Husband, A.J. *Flavonoid compounds in maintenance of prostate health and prevention and treatment of cancer*. Mol Biotechnol 2005, 30(3): 253-70.
22. Agüero, M.F., Facchinetti, M.M., Shelag, Z. et al. *Phenoxodiol, a novel isoflavone, induces G1 arrest by specific loss in cyclin-dependent kinase 2 activity by p53-independent induction of p21WAF1/CIP1*. Cancer Res 2005, 65(8): 3364-73.
23. Sapi, E., Alvero, A.B., Chen, W. et al. *Resistance of ovarian carcinoma cells to docetaxel is XIAP dependent and reversible by phenoxodiol*. Oncol Res 2004, 14(11-12): 567-78.
24. Alvero, A.B., Brown, D., Montagna, M. et al. *Phenoxodiol-topotecan coadministration exhibit significant anti-tumor activity without major adverse side effects*. Cancer Biol Ther 2007, 6(4): 612-7.
25. Chou, T.C., Talalay, P. *Quantitative analysis of dose-effect relationships: The combined effects of multiple drugs or enzyme inhibitors*. Adv Enzyme Regul 1984, 22: 27-55.
26. Kanzawa, F., Nishio, K., Fukuoka, K., Fukuda, M., Kunimoto, T., Saijo, N. *Evaluation of synergism by a novel three-dimensional model for the combined action of cisplatin and etoposide on the growth of a human small-cell lung-cancer cell line, SBC-3*. Int J Cancer 1997, 71(3): 311-9.
27. Cheng, J.Q., Jiang, X., Fraser, M. et al. *Role of X-linked inhibitor of apoptosis protein in chemoresistance in ovarian cancer: Possible involvement of the phosphoinositide-3 kinase/Akt pathway*. Drug Resist Updat 2002, 5(3-4): 131-46.
28. Li, J., Sasaki, H., Sheng, Y.L. et al. *Apoptosis and chemoresistance in human ovarian cancer: Is Xiap a determinant?* Biol Signals Recept 2000, 9(2): 122-30.
29. Reed, J.C. *Apoptosis-based therapies*. Nat Rev Drug Discov 2002, 1(2): 111-21.
30. Asselin, E., Mills, G.B., Tsang, B.K. *XIAP regulates Akt activity and caspase-3-dependent cleavage during cisplatin-induced apoptosis in human ovarian epithelial cancer cells*. Cancer Res 2001, 61(5): 1862-8.
31. Mor, G., Montagna, M.K., Alvero, A.B. *Modulation of apoptosis to reverse chemoresistance*. Methods Mol Biol 2008, 414: 1-12.
32. Finlayson, K., Turnbull, L., January, C.T. et al. *[³H]Dofetilide binding to HERG transfected membranes: A potential high throughput preclinical screen*. Eur J Pharmacol 2001, 430(1): 147-8.
33. Choueiri, T.K., Mekhail, T., Hutson, T.E. et al. *Phase I trial of phenoxodiol delivered by continuous intravenous infusion in patients with solid cancer*. Ann Oncol 2006, 17(5): 860-5.
34. ten Bokkel, H.W., Lane, S.R., Ross, G.A. *Long-term survival in a phase III, randomised study of topotecan versus paclitaxel in advanced epithelial ovarian carcinoma*. Ann Oncol 2004, 15(1): 100-3.
35. Ghamande, S., Lele, S., Marchetti, D. et al. *Weekly paclitaxel in patients with recurrent or persistent advanced ovarian cancer*. Int J Gynecol Cancer 2003, 13(2): 142-7.